Digest Journal of Nanomaterials and Biostructures Vol. 15, No. 2, April - June 2020, p. 299 - 309

STUDY ON PREPARATION AND PROPERTIES OF PVA/AgNPs COMPOSITE NANOFIBER MASK MATERIAL

Z. XIANHUA[a,*], F. XIANGWEI[a], Y. BIN[a], L. FAN[b], C. LINA[a], Z. CENGCENG[a]
[a]*School of Textiles, Henan University of Engineering, Zhengzhou 450007, China*
[b]*College of Textiles, Zhongyuan University of Technology, Zhengzhou 450007, China*

In this paper, the preparation and properties of polyvinyl alcohol (PVA)/silver nanoparticles (AgNPs) composite nanofiber mask material were studied. Firstly, PVA spinning solution was prepared, and PVA nanofibers with different mass fractions (5 wt%, 7 wt%, 8 wt%, 9 wt% and 11 wt%) were prepared by electrospinning technology. The morphology of PVA nanofibers was observed under electron microscope, and the results showed that 8 wt% PVA nanofibers had the best morphology. AgNPs with different mass fractions (0.02 wt%, 0.03 wt%, 0.04 wt%, 0.05 wt% and 0.06 wt%) were dispersed in pure water and blended with 8 wt% PVA solution to prepare PVA/AgNPs composite nanofibers by electrospinning. The effects of different mass fractions of AgNPs on the morphology of PVA/AgNPs composite nanofibers were analyzed. Infrared spectroscopy and X-ray diffraction were used to test the PVA/AgNPs composite nanofibers. PVA/AgNPs composite nanofiber mask fabric was prepared by using activated carbon nonwoven fabric as substrate. The filterability, air permeability and moisture permeability of PVA/AgNPs composite nanofiber mask material were tested and analyzed. The result showed that PVA/AgNPs composite nanofiber mask material has good filtration, moisture permeability and air permeability, and has broad application prospects.

(Received October 21, 2019; Accepted April 4, 2020)

Keywords: PVA/AgNPs, Nanofibers, Morphology, Mask, Performance

1. Introduction

Polyvinyl alcohol (PVA) is non-toxic and biocompatible. It is easy to obtain nanofibers [1-4]. There are many literatures on PVA nanofibers, including spinnability of different types of PVA, selection of spinning conditions and preparation of PVA composite fibers [5-6].

AgNPs is a kind of silver (Ag) with nano-size, insoluble in water and not easy to volatilize. Ag is a natural inorganic antimicrobial agent, which not only kills many kinds of bacteria, but also has the same killing ability to resistant bacteria [7-8]. Trace silver mixed with polymers has a strong bactericidal ability [9-10], it can bind closely with the body, so as to ensure the persistence of antimicrobial effect.

* Corresponding author: xianhuaz@haue.edu.cn

The nanofibers prepared by electrospinning have excellent morphology and the electrospinning equipment is simple [11-13]. They can be well controlled from the range of raw materials to the possibility of industrial production [14]. The polymer solution is charged by high voltage electrostatic force. The droplets at the needle position are subjected by the electric field force to form a jet, which evaporates and solidifies during the injection process to form a fiber felt [15-17]. In recent years, with the continuous efforts of many experts and scholars, electrospinning technology has been greatly developed and improved [18]. In recent years, nanofibers have great development prospects in protection, such as military protective clothing, industrial protective clothing and haze masks [19-20]. The nano-material has smaller diameter, higher filtration efficiency and higher moisture permeability [21-23], so the nano-mask material with anti-haze effect has broad prospects and benefits [24]. In this paper, PVA/AgNPs electrospinning composite nanofibers membrane with filter layer was prepared. The filtration, air permeability and moisture permeability of PVA/AgNPs composite nanofiber mask material were tested. The composite nanofibers mask with this structure is non-toxic, non-polluting and has good performance.

2. Experiment

2.1. Material

1797 PVA (Aladdin): alcoholysis degree 96.0-98.0%; AgNPs (Aladdin), diameter 60-120 nm, molecular weight 107.87; ultra-pure water was prepared by WP-UP-WF-40 micro-analysis ultra-pure water machine.

2.2. Experimental instruments

DF-101S collector constant temperature heating magnetic stirrer, SYU-3-100D ultrasound, D-ES5OPN-1OW/DDPM electrostatic high voltage generator, WZ-50C6 injection pump, HH-4 digital constant temperature water bath.

2.3. Preparation of PVA Solution

The 5 g, 7 g, 8 g, 9 g and 11 g of PVA were weighed and the pure water of 95 g, 93 g, 92 g, 91 g and 89 g were put into the blue bottle cap, respectively. The samples of PVA were swelled at room temperature for 45 minutes and then heated in HH-4 digital thermostat water bath at 98 ℃. After 4 hours, they were taken out and cooled at room temperature for 50 minutes.

2.4. Preparation of PVA/AgNPs Solution

0.02 g, 0.03 g, 0.04 g, 0.05 g and 0.06 g AgNPs were weighed in blue cap bottles, then 91.98 g, 91.97 g, 91.96 g, 91.95 g and 91.94 g of pure water were weighed, respectively. AgNPs samples were dispersed by ultrasound for 45 minutes and then magnetic stirring was carried out by magnetic stirrer for 30 minutes. Five 8 g PVA were weighed and put into AgNPs solution. The samples were swelled at room temperature for 45 minutes. The samples were heated at 98 ℃ in HH-4 constant temperature water bath for 4 hours. Finally, the samples were cooled at room temperature for use.

2.5. Preparation of Nanofiber Membrane

A syringe was used to absorb 5 ml spinning solution and fixed on the spinning pump. Needle No.19 was connected with the positive pole of the power supply and the receiving screen was connected with the negative pole. The spinning distance was 15 cm, the voltage was 16 kV and the spinning speed was 1.5 ml/h. After spinning for 4 hours, the nanofibers were taken off and dried in a constant temperature oven at 60 ℃ for 6 hours. Samples of nanofibers and mask materials can be obtained.

2.6. SEM Analysis

Electron microscopy tests were carried out using Sigma 500 scanning electron microscopy produced by Carl Zeiss, Germany. The samples were cut into suitable size and pasted on the sample table. The samples were sprayed using gold with vacuum coating machine for 30 seconds. Finally, the samples were tested by electron microscopy and the SEM images were saved.

2.7. Infrared Spectrum

Nicolet 6700 Fourier Transform Infrared Spectrometer of Thermo Fisher Company, USA, has a wavenumber range of 250-4500 cm^{-1} and a resolution of 0.09 cm^{-1}. Fourier transform infrared spectroscopy (FTIR) was used to measure the total reflection. Then the data were processed by Origin 8.0 and the infrared absorption peaks of PVA/AgNPs composite nanofibers were analyzed.

2.8. X-ray Diffraction Analysis

The D8 ADVANCE X-ray diffractometer of Bruker Company in Germany was used. The scanning angle was 10 ° to 50 ° and the scanning speed was 5 °/min.

2.9. Preparation of Nano-fiber Mask Material

Activated carbon substrate was pasted on the receiving screen, and different mass ratios PVA/AgNPs were prepared. The nanofibers were spun on the activated carbon substrate by electrospinning technology.

2.10. Filtration Performance

The TSI 8130 automatic filter material detector of TSI Company in the United States adopts NaCl aerosol with median diameter of 0.075+0.020 um. The gas flow range was 0-100 L/min, sample test area was 100 cm^2 and the gas flow rate was 32 L/min.

2.11. Air permeability

YG461Z fully automatic air permeability tester with pressure of 100 Pa and experimental area of 20 cm^2 was used. The average value of each sample was measured 10 times.

2.12. Moisture permeability

YG601H-II computerized fabric moisture permeameter was used. The conditions for testing was the relative humidity of 90% at 38 ℃for 1 h.

3. Results and analysis

3.1. Morphology of Nanofiber Membrane

The morphology of PVA nanofibers with different mass fractions was analyzed, and the optimum mass fraction was obtained. The PVA/AgNPs composite nanofibers were prepared by blending 8 wt% PVA with 0.02 wt%, 0.03 wt%, 0.04 wt%, 0.05 wt% and 0.06 wt% AgNPs, respectively.

3.1.1. Morphology of PVA nanofibers

Fig. 1 a is the electron microscopic image of 5 wt% PVA nanofibers. There are a large number of beads in nanofibers through electron microscopic observation. The fibers are uneven in thickness, largely different in diameter and have more fiber adhesion. This may be due to the fact that when the mass fraction of PVA is low, the number of PVA molecules in the same mass solution is few and the viscosity is low, which leads to the appearance of beads.

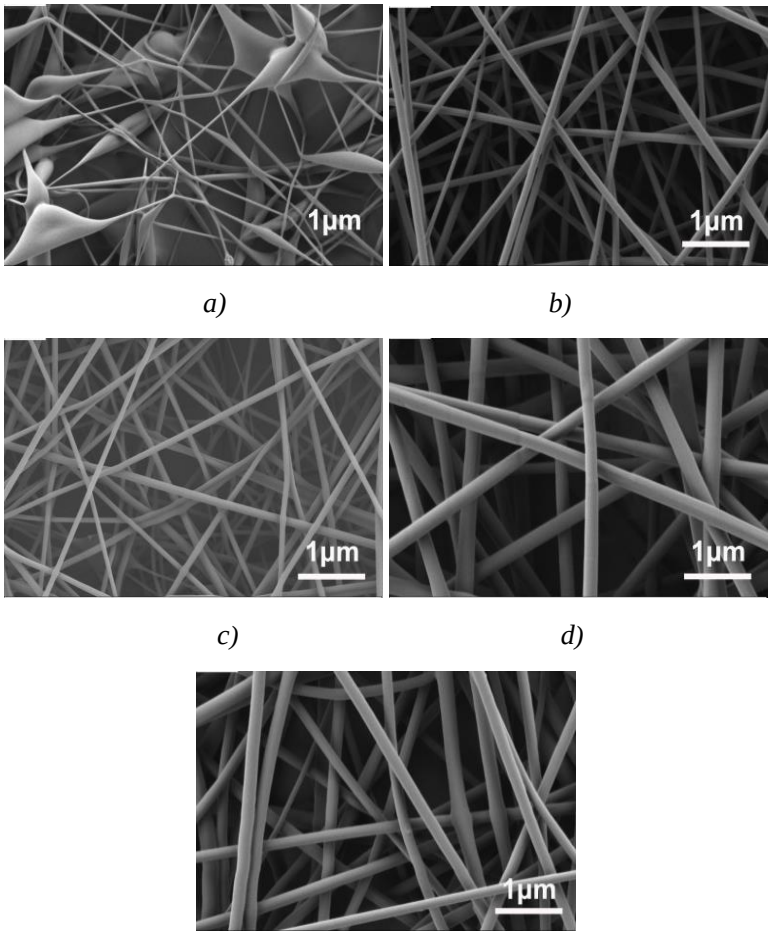

a) *b)* *c)* *d)* *e)*

Fig. 1. Electron microscopy of PVA nanofibers with different mass fractions a 5 wt%; b 7 wt%; c 8 wt%; d 9 wt%; e 11 wt%.

When the mass fraction of PVA increases to support the continuous elongation of jet, which can support the continuous elongation of jet in spinning, the beads and adhesion will not

occur. 7 wt% PVA nanofibers have uniform diameter and good morphology, but a small amount of adhesion and beads are observed under low magnification microscopy in Fig. 1b. The PVA nanofibers in Fig. 1c, 1d and 1e are well formed and there are no defects in the nanofibers. PVA nanofibers have thin diameter and are uniform through observation in Fig. 1c. PVA nanofibers have larger diameter in Fig. 1d and 1e. These three kinds of PVA nanofibers have good morphology without obvious irregular adhesion and spindle.

In order to further study the effect of different mass fractions on the morphology of PVA nanofibers, the diameter of PVA nanofibers was measured by Image J, and the average value of each sample was measured 100 times, as shown in Table 1.

Table 1. Average diameter and standard deviation of PVA nanofibers with different mass fractions.

PVA mass fraction	7	8	9	11
average diameter	130	158	316	349
standard deviation	21	20	47	51

From Table 1, the average diameter of fibers increases with the increase of PVA mass fraction and showed a positive correlation. The average minimum diameter of fibers is 130 nm, and the average maximum diameter of fibers is 349 nm. With the increase of the mass fraction of PVA solution, the more the number of PVA molecules and the entanglement between molecular chains in a certain mass solution, the higher the viscosity of the solution. It is difficult to stretch and refine the fibers and coarsens the diameter of the fibers. The increase of diameter standard deviation of PVA nanofibers may be due to the uneven distribution of entanglement between molecular chains of PVA. The minimum diameter standard deviation of PVA nanofibers is 21, and the maximum diameter standard deviation of PVA nanofibers is 51. Under the condition of smooth surface of nanofibers, the smaller the average diameter and standard deviation of nanofibers, the better the morphology of nanofibers. According to Fig. 1 and Table 1, 8 wt% PVA is the best spinning concentration under the same experimental conditions.

3.1.2 Morphology of PVA/AgNPs Composite Nanofibers

Fig. 2 shows that PVA/AgNPs composite nanofibers with different mass ratios are well formed. The surface without concave-convex is smooth. The diameter of PVA/AgNPs composite nanofibers with different mass ratios is different and the specific differences are further analyzed, as shown in Table 2.

Table 2. Average diameter and standard deviation of PVA/AgNPs composite nanofibers with different mass ratios.

PVA/AgNPs mass ratio	8:0.02	8:0.03	8:0.04	8:0.05	8:0.06
average diameter	151	159	197	206	207
standard deviation	22	31	32	34	40

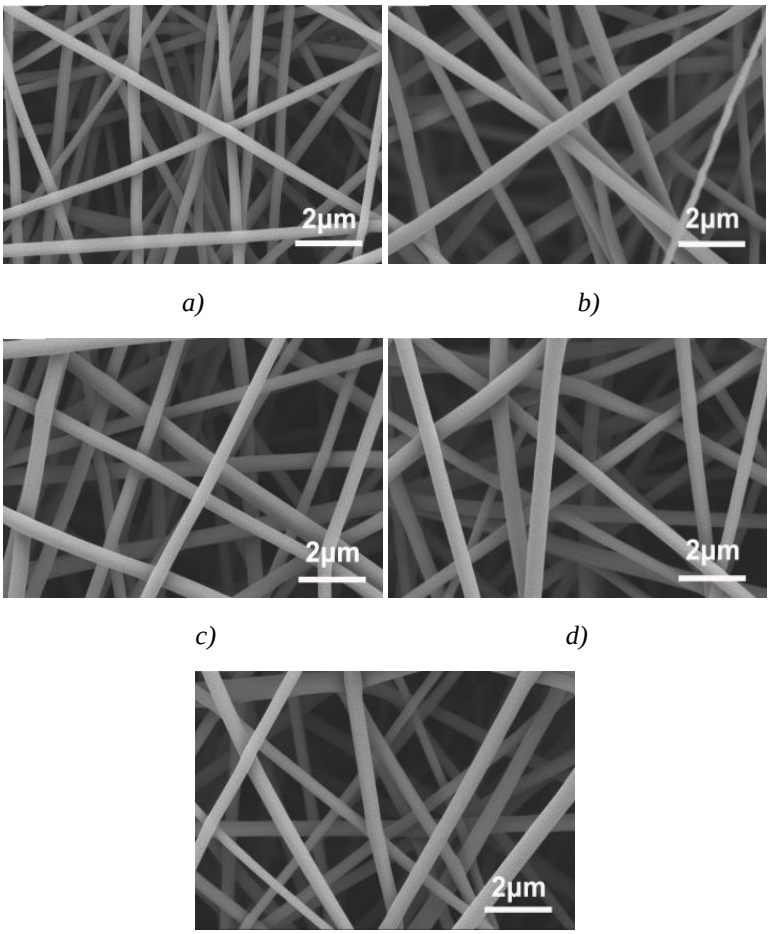

Fig. 2. Electron microscopy of PVA/AgNPs composite nanofibers with different mass ratios a 8:0.02; b 8:0.03; c 8:0.04; d 8:0.05; e 8:0.06.

Table 2 shows that with the increase of AgNPs mass fraction in the PVA/AgNPs composite nanofibers, the average diameter and standard deviations increase. The minimum and maximum average diameters of PVA/AgNPs composite nanofibers are 151 and 207 nm, respectively. The minimum and maximum diameter standard deviations of PVA/AgNPs composite nanofibers are 22 and 40, respectively.

The reason for the increase of diameter of PVA/AgNPs composite nanofibers may be that the conductivity of PVA/AgNPs mixed solution increases with the increase of mass fraction of AgNPs, which leads to the increase of spinning speed, and the diameter becomes thicker.

3.2. Infrared Spectrum Analysis

Fig. 3 shows that pure PVA nanofibers have six characteristic peaks at 834.56, 1087.19, 1324.88, 1419.86, 2939.28 and 336.05 cm^{-1}. Fig. 4 shows infrared spectra of PVA/AgNPs composite nanofiber membranes with different mass ratios.

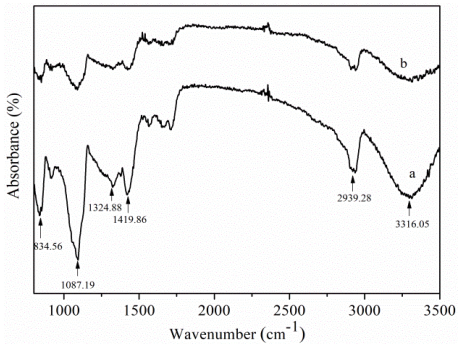

Fig. 3. Infrared spectra of 8 wt% PVA and 8/0.06 PVA/AgNPs nanofibers a 8:0.06; b 8:0.00.

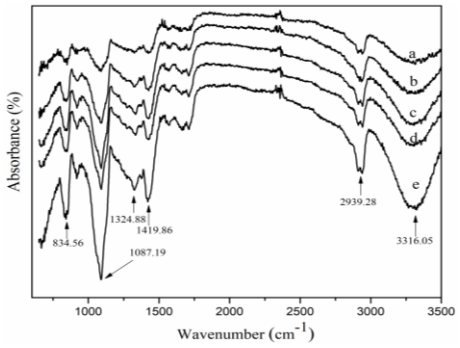

Fig. 4. Infrared spectra of PVA/AgNPs composite nanofiber membranes with different mass ratios a 8:0.02; b 8:0.03; c 8:0.04; d 8:0.05; e 8:0.06.

No new peaks appear in PVA/AgNPs composite nanofiber membranes adding AgNPs. The shape of absorption peaks of PVA/AgNPs composite nanofiber membranes are similar. However, with the increase of AgNPs, the infrared spectral signals of the peaks increase.

3.3. X-ray Diffraction

The diffraction curves of PVA/AgNPs composite nanofibers with different mass ratios have similar laws in Fig. 5. The same characteristic peaks of PVA/AgNPs composite nanofibers appear near the diffraction angles of 13.60˚, 29.18˚ and 40.93˚. The diffraction angle disappears at 18.53˚ and the diffraction signal increases at 13.60˚ after adding AgNPs. It is inferred that the interaction between AgNPs and PVA molecules may occur.

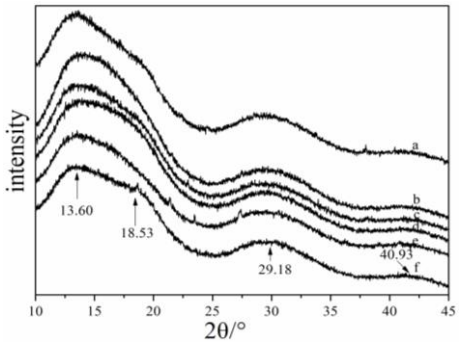

Fig. 5. X-ray diffraction patterns of PVA and PVA/AgNPs composite nanofibers a 8:0.06; b 8:0.05; c 8:0.04; d 8:0.03; e 8:0.02; f 8:0.00.

3.4. Filterability

The filterability of PVA/AgNPs composite nanofiber mask material with different mass ratios was tested. The average value of each material was measured 3 times, and the data were shown in Table 3.

Table 3. Filtration of PVA/AgNPs composite nanofiber mask materials with different mass ratios.

Category	8:0.00	8:0.02	8:0.03	8:0.04	8:0.05	8:0.06
	89.90	90.12	90.90	90.58	91.20	92.70
Filtration efficiency（%）	86.50	90.17	90.55	90.50	91.40	92.90
	79.00	90.40	90.79	90.60	91.30	92.20
Average filtration efficiency （%）	85.13	90.23	90.75	90.56	91.30	92.60

Table 3 shows that the filtration performance of PVA/AgNPs composite nanofiber mask material is significantly improved compared with that of 8 wt% PVA nanofiber mask material. This is maybe that AgNPs improve the solution conductivity and the spinning speed is accelerated, so mask material becomes thicker and the filtration performance is enhanced in the same time. When the mass ratio of PVA/AgNPs is 8:0.06, the filtration efficiency is 92.60%, and the filtration performance is the best.

3.5. Air permeability

The air permeability of PVA/AgNPs composite nanofiber mask materials with different mass ratios was tested. Each sample was measured 10 times to get the average value, the data were shown in Table 4.

Table 4. Permeability of PVA/AgNPs composite nanofiber mask material with different mass ratios.

Unit: mm/s

Category / Serial number	8:0.06	8:0.05	8:0.04	8:0.03	8:0.02	8:0.00
1	155	166	167	168	172	180
2	154	165	168	168	177	179
3	157	162	168	164	178	181
4	154	169	165	168	175	179
5	155	164	169	169	174	180
6	153	165	168	170	175	178
7	154	168	169	171	179	180
8	151	168	169	167	176	179
9	155	166	167	169	177	181
10	156	164	167	170	178	180
Average value	154.4	165.7	167.7	168.4	176.1	179.7

Table 4 shows that the air permeability of PVA/AgNPs composite nanofiber mask material decreases gradually with the increase of AgNPs content. The best air permeability is PVA/AgNPs (8:0.00) mask material with 179.7 mm/s. The worst air permeability is PVA/AgNPs (8:0.06) composite nanofiber mask material with 154.4 mm/s.

The main reason may be that AgNPs have conductivity. The conductivity of the solution increases as the mass fraction of AgNPs increasing. The spinning speed of nanofibers increases at the same time. so the mask materials become thick and the permeability decreases accordingly.

3.6. Moisture permeability

The moisture permeability of PVA/AgNPs composite nanofiber mask materials with different mass ratios was tested. The average value of each fabric was measured 3 times, as shown in Table 5.

Table 5. Moisture permeability of PVA/AgNPs composite nanofiber mask material with different mass ratios.

Category	Mass before moisture permeability g	mass after moisture permeability g	Weight difference g	Moisture permeability g/d*m^2	Average moisture permeability g/d*m^2
8:0.00	181.018	181.434	0.416	2595.61	2570.65
	182.391	182.798	0.407	2539.45	
	181.555	181.968	0.413	2576.89	
8:0.02	181.859	182.277	0.418	2608.09	2676.72
	181.766	182.194	0.428	2670.48	
	181.896	182.337	0.441	2751.59	
8:0.03	184.451	184.919	0.468	2920.06	2886.78
	188.439	188.877	0.438	2732.87	
	189.952	190.334	0.482	3007.41	
8:0.04	184.384	184.817	0.433	2701.68	2761.66
	188.597	189.010	0.413	2575.89	
	184.237	184.723	0.486	2576.89	
8:0.05	187.126	187.563	0.437	2726.63	2909.66
	174.016	174.498	0.482	3007.41	
	175.112	175.592	0.480	2994.93	
8:0.06	189.309	189.764	0.455	2838.95	3073.97
	171.893	172.364	0.471	2938.78	
	185.434	185.986	0.552	3444.17	

Table 5 shows that the moisture permeability of PVA/AgNPs composite nanofiber mask material is enhanced compared with PVA nanofibers. The moisture permeability of 8 wt% PVA nanofiber mask material is the smallest. With the increase of AgNPs content, the moisture permeability of PVA/AgNPs composite nanofiber mask materials show an overall upward trend.

4. Conclusion

PVA/AgNPs composite nanofibers were successfully spun by electrospinning technology, and the PVA composite nanofiber mask material was prepared using activated carbon substrate. Scanning electron microscopy showed that 8 wt% PVA nanofibers had the best morphology. PVA/AgNPs composite nanofibers with different mass ratios are well formed. The filtration efficiency and resistance pressure drop of PVA/AgNPs composite nanofiber mask material were tested by automatic filter material detector. 8 wt% PVA nanofiber mask material had the lowest filtration performance under the same spinning time of 4 h. The filterability of PVA/AgNPs composite nanofiber mask material was significantly improved by adding different mass fraction of AgNPs. With the increase of AgNPs mass fraction, the PVA/AgNPs composite nanofiber layer

becomes thicker, which results in the corresponding increase of mask material thickness and the decrease of air permeability. With the increase of AgNPs mass fraction, the moisture permeability of PVA/AgNPs composite nanofibers masks increased. Under this experimental condition the moisture permeability of 8 wt% PVA was the lowest and that of PVA/AgNPs (8:0.06) was the highest.

Acknowledgements

The authors gratefully acknowledge Henan University of Engineering Doctoral Fund Project (D2017005), Henan Province Science and Technology Research Project (182102310862), Collaborative Innovation Center of Textile and garment industry, Henan Province and Henan Provincial Higher Education Key Research Project Plan (17B540003).

References

[1] R. Purwar, S. Sharma, P. Sahoo et al., Fibers & Polymers **16**(4), 761 (2015).
[2] M. Zhang, Y. J. Liu, T. Y. Xu et al., Advanced Materials Research **332-334**, 1472 (2011).
[3] H. Itoh, Y. Li, K. H. K. Chan et al., Polymer Bulletin **73**(10), 2761 (2016).
[4] L. Jia, X. H. Qin, Journal of Thermal Analysis and Calorimetry **112**(2), 595 (2013).
[5] F. Hejazi, S. M. Mousavi, Desalination & Water Treatment **57**(5), 1959 (2016).
[6] Z. L. Cheng, X. X. Qin, Z. Liu et al., Polymers for Advanced Technologies **28**(6), 52 (2017).
[7] M. Heshmati, S. Arbabibidgoli, S. Khoei et al., Iranian Journal of Pharmaceutical Research Ijpr **14**(4), 1171 (2015).
[8] N. K. Ahila, V. S. Ramkumar, S. Prakash et al., Biomedicine & Pharmacotherapy **84**, 60 (2016).
[9] O. Eren, N. Ucar, A. Onen et al., Journal of Composite Materials **50**(15), 2073 (2016).
[10] H. Xue, Y. Zhang, B. Zhang et al., Transactions of the Chinese Society of Agricultural Engineering **257**(9), 4524 (2018).
[11] X. Cui, M. Yu, C. Wang et al., Polymer Science **58**(3), 357 (2016).
[12] M. Mirjalili, S. Zohoori, Journal of Nanostructure in Chemistry **6**(3), 1 (2016).
[13] J. Xue, J. Xie, W. Liu et al., Accounts of Chemical Research **50**(8), 1976 (2017).
[14] B. Robb, B. Lennox, Electrospinning for Tissue Regeneration, 51 (2011).
[15] J. Kim, J. P. Hinestroza, W. Jasper et al., Fibers & Polymers **12**(1), 89 (2011).
[16] F. Marchi, R. Dianoux, H. Smilde et al., Journal of Electrostatics **66**(9), 538 (2008).
[17] P. A. Cox, M. S. Glaz, J. S. Harrison et al., Journal of Physical Chemistry Letters **6**(15), 2852 (2015).
[18] H. Y. Mi, X. Jing, H. X. Huang et al., Materials Letters **204**, 45 (2017).
[19] G. Yin, Q. Zhao, Y. Zhao et al., Journal of Applied Polymer Science **128**(2), 1061 (2013).
[20] P. Otrisal, V. Obsel, J. Buk et al., Nanomaterials **8**(564), 1 (2018).
[21] S. Zhang, W. S. Shim, J. Kim, Materials & Design **30**(9), 3659 (2009).
[22] Yu Tian, Yun Liang, Yan Cui et al., Advanced Materials Research **335-336**(24), 411 (2011).
[23] Y. U. Qin, B. Deng, Q. Liu et al., Journal of Textile Research **34**(11), 77 (2013).
[24] H. W. Huang, C. C. Kao, T. H. Hsueh et al., Materials Science & Engineering B **113**(2), 125 (2004).